On wire-corrector optimization in the HL-LHC and the appearance of special aspect ratios

D. Kaltchev*

TRIUMF, 4004 Wesbrook Mall, Vancouver, B.C., Canada V6T 2A3

(Dated: Apr 1 2021)

* kaltchev@triumf.ca kaltchev@cern.ch

1. INTRODUCTION

Two-dimensional amplitude-independent Resonance Driving Terms (RDT), based on the coefficients c_{pq} in the multipole expansion of the beam-beam kick, have been used in [1] to describe the effects of long-range (l.r.) beam-beam interactions in the HL-LHC and optimization of wire correctors. The RDT represent a powerful tool to investigate the effect of beam-beam and its compensation since, by combining the above coefficients with the betatronic phases (in the same way as this is done for lattice multipoles) they account for the lattice symmetries.

In [1], a common expression is used for both the l.r. beam-beam encounter (bb) and the wire corrector (infinite and thin wire) and an analytic formula is found that produces the optimum parameters of the wires. The formula follows from imposing the condition for simultaneous cancellation of a target pair RDT (indices p_1, q_1, p_2, q_2) and gives, for a fixed location of the wire left-right symmetric wrt the IP, two equal optimum parameters: integrated current and distance to the axis. These guarantee that the target pair, and also a symmetric one (q_1, p_1, q_2, p_2), will vanish over a single turn. Further, by varying the wire location, it turns out that many, in fact nearly all, other RDT (arbitrary indices p, q) can be cancelled, if only the wires are installed very close to longitudinal locations that correspond to two special values of the beta-function aspect ratio $\frac{\beta_{x,y}}{\beta_{y,x}} =$ 1/2 and 2. Section 2 focuses on the above formula, attempting to explain the appearance of these special values.

Note: The paper is seen as first step in a study that aims to include the dependence on weak-beam-particle amplitude $a_{x,y}$, i.e on the transverse horizontal and vertical displacements x, y of the weak-beam particle from the weak beam core. The RDT approach is amplitude-independent in a sense that the above dependence is naturally captured in the high-order terms in the expansion parameter – interactions occurring far from the weak-beam axis (and hence close to the strong beam core) correspond to taking high-orders of x, y. It therefore represents an interest to reproduce the above results using Hamiltonian approach, i.e. Hamiltonian Fourier coefficients and the corresponding *amplitude-dependent* Hamiltonian Driving Terms (HDT). These coefficients are denoted with $C_{pq} = i^{p+q} D_{pq}$, where D is a real quantity. Thus, in the Hamiltonian approach, the beam-beam kick is replaced by the corresponding potential. Higher orders of x, y are accounted for via the exact functions $C_{pq}(a_x, a_y)$. The idea is that the driving term cancellation derived below could be verified for amplitudes up to the strong beam core.

2. WIRE CORRECTION USING RDT

Here first the wire-correction formula is revisited. Then, expression for the residual RDT as a function of the *sigma* aspect ratio r is then derived. Imposing the condition that the residual RDT is cancelled for arbitrary indices produces the special, a.k.a. magic, values of r: $r \approx 1/\sqrt{2}$ and $\sqrt{2}$, corresponding to $r^2 \approx 1/2$ and 2 – the *beta* aspect ratios found in [1].

The optics functions chosen are r, as defined above, $\sqrt{\beta_{x,y}}$ of the weak beam (same as in [1]) and the normalized separation in the x-plane (in IR5). These appear as vectors: $\boldsymbol{r}$, $\boldsymbol{\sigma}$ and $\boldsymbol{\psi}$ respectively as they are naturally discrete (index n). In particular, for a driving term, the components of $\boldsymbol{\psi}$ are needed at the longitudinal locations of the bb collisions s_n spaced half-bunch distance 3.75 m apart. The vectors will be operated upon "by component" – for example raised to an integer power. In [1], the analogous three discrete quantities are the real separation in the y-plane and the two weak-beam beta functions (in IR1).

Using the same spacing, we extend the above vectors to include the wire domain ("w"), i.e. we define a "slot" at which there is either a bb encounter, or a wire may be located. If some result appears as a smooth functions of the parameters (say r), then plots are made by simply mapping this function over the wire domain of the vector(s).

Specifically, we consider IR5 and denote with $2 \times N_{bb}$ (in our example $= 2 \times 18$) the number of l.r. bb collisions. There are then 2×54 slots extending left and right of IP5 over a distance $s \approx \pm 200$ m from IP5. Same as in [1], from the insertion symmetry it will follow that using only the "R" slots (these on the right of IP5) is sufficient. To summarize, in general three vectors of length 54 provide a full description of the wire-correction problem and each vector has two parts – a beam-beam domain (index bb), of length N_{bb}, and a wire domain (index w).

A. RDT

A round-beam (at the IP) optics is assumed with emittance ε equal in both planes. For this section we take $\varepsilon = 1$. The notations are meant to provide some link with the next section.

Using the anti-symmetry of the optics let us rewrite the (p,q)-coefficient c_{pq} in the expansion of the kick, delivered to the weak-beam particle by either a single bb or a wire corrector, in the following way: denote

$$\psi_x = \frac{|\mathsf{D}_x|}{\sigma_x}, \quad \psi_y = \frac{|\mathsf{D}_x|}{\sigma_y}; \quad \sigma_{x,y} \equiv \sqrt{\beta_{x,y}}, \tag{2.1}$$

where $\beta_{x,y}$ and D_x are the lattice parameters: weak-beam beta function and real space separation. Then, for the n-th slot [1]

$$c_{pq}^{(n)} = \frac{{\beta_x^{(n)}}^{\frac{p}{2}} {\beta_y^{(n)}}^{\frac{q}{2}}}{|{\mathsf{D}_x}^{(n)}|^{p+q}} = ({\psi_x^{(n)}})^{-p}\ ({\psi_y^{(n)}})^{-q} \tag{2.2}$$

where for a wire slot (n) is replaced with w. The lattice parameters appear as L-R pairs and within each pair: $\sigma_{x,y}^{(n),\mathrm{L}} = \sigma_{y,x}^{(n),\mathrm{R}}$, ${\mathsf{D}_x}^{(n),\mathrm{L}} = -{\mathsf{D}_x}^{(n),\mathrm{R}}$ and hence $\psi_{x,y}^{(n),\mathrm{L}} = \psi_{y,x}^{(n),\mathrm{R}}$. Only the absolute value $|\mathsf{D}_x|$ participates – this accounts for the π phase jump from left to right [1] – so that all ψ are positive.

By summing over the bb slots, the RDT (c_{pq}^{LR} in [1]) is

$$\begin{aligned}
\Sigma_{pq} &= \sum_{n\in\mathrm{LR}} {\psi_x^{(n)}}^{-p} {\psi_y^{(n)}}^{-q} = \\
&= \sum_{n\in\mathrm{R}} {\psi_x^{(n)}}^{-p} {\psi_y^{(n)}}^{-q} + \sum_{n\in\mathrm{L}} {\psi_x^{(n)}}^{-p} {\psi_y^{(n)}}^{-q} = \\
&= \sum_{n\in\mathrm{R}} ({\psi_x^{(n)}}^{-p} {\psi_y^{(n)}}^{-q} + {\psi_y^{(n)}}^{-p} {\psi_x^{(n)}}^{-q}) = \\
&= \boldsymbol{\psi}_L^{-p} \cdot \boldsymbol{\psi}_R^{-q} + \boldsymbol{\psi}_R^{-p} \cdot \boldsymbol{\psi}_L^{-q}
\end{aligned} \tag{2.3}$$

The third line follows from the second, because each term in the L sum has a corresponding one in the R sum with $x \leftrightarrow y$. In the fourth line x and y are replaced with L and R and further ψ_{L}, ψ_{R} are the components of corresponding vectors (in bold). Bringing a vector to a power is understood to be "by component". Thus the RDT depends on two vectors $\boldsymbol{\psi}_L$ and $\boldsymbol{\psi}_R$ of length 18 with components the values of $\psi_{\mathrm{L}} = \frac{\mathsf{D}}{\sigma_x^{\mathrm{L}}}$, $\psi_{\mathrm{R}} = \frac{\mathsf{D}}{\sigma_x^{\mathrm{R}}}$ ($\mathsf{D} \equiv {\mathsf{D}_x}^{\mathrm{R}} > 0$) over IR5 Right. The vectors are different since outside the drift region $\sigma_x^{\mathrm{R}} \neq \sigma_x^{\mathrm{L}}$. Alternatively, one can replace one of them by $\boldsymbol{r}$, whose components are the sigma aspect ratios $r \equiv \sigma_x^{\mathrm{R}}/\sigma_x^{\mathrm{L}} = \psi_{\mathrm{L}}/\psi_{\mathrm{R}}$. If we denote $\boldsymbol{\psi} \equiv \boldsymbol{\psi}_L$, then the RDT (2.3) can then be rewritten as

$$\begin{aligned}
\Sigma_{pq} &= \sum_{n\in\mathrm{R}} {\psi_n}^{-(p+q)} (r_n^p + r_n^q) = \\
&= \boldsymbol{\psi}^{-(p+q)} \cdot (\boldsymbol{r}^p + \boldsymbol{r}^q).
\end{aligned} \tag{2.4}$$

Since in the wire domain, ψ is simply proportional to r in fact Σ_{pq} depends only on one of the vectors, say $\boldsymbol{r}$, plus one constant (see also [1]). Another vector, not participating in the driving term, is $\boldsymbol{\sigma}$ with components $\sigma_{\mathrm{L}} \equiv \sigma_x^{\mathrm{L}}$.

We now extend the length of the three vectors to 54 to include the wire domain. Figure 1 and Table (2.5) show $\boldsymbol{\psi}$ and $\boldsymbol{r}$. The extreme, i.e. minimum and maximum values, for of r_n are 0.48 and 1.56.

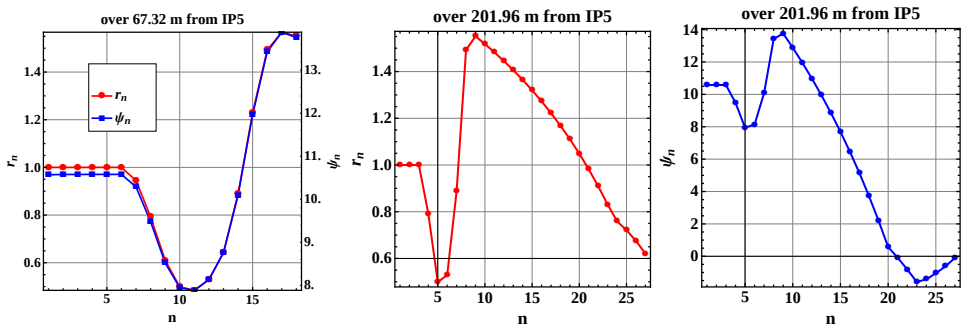

FIG. 1. Components of the vectors: sigma aspect-ratio $\boldsymbol{r}$ and normalized separation $\boldsymbol{\psi}$ over the right half of IR5. Left plot: over the bb domain (18 slots), where ψ is proportional to r; Right: over the full domain – bb and wire (double spacing is used).

$$\begin{array}{lccccccccccccccccc} \boldsymbol{\psi} = (& 10.57 & 10.57 & 10.57 & 10.57 & 10.57 & 10.57 & 10.28 & 9.48 & 8.52 & 7.94 & 7.88 & 8.13 & 8.75 & 10.09 & 11.96 & 13.42 & 13.88 & 13.75\ ) \\ \boldsymbol{r} = (& 1. & 1. & 1. & 1. & 1. & 1. & 0.94 & 0.79 & 0.61 & 0.49 & 0.48 & 0.52 & 0.64 & 0.88 & 1.22 & 1.49 & 1.56 & 1.55\ ) \end{array} \tag{2.5}$$

B. Wire correction and residual RDT

Below we will use three Σ_{pq} (a triad of RDT). One is given by (2.4). Another two are $\Sigma_{p_1q_1}$ and $\Sigma_{p_2q_2}$ (with corresponding replacements of p and q). As explained above, the plan is to first compute the two wire parameters $N^{\mathrm{w}}(r)$ and $\mathsf{D}^{\mathrm{w}}(r)$ that follow from the condition that the target pair p_1, q_1 is p_2, q_2 is simultaneously cancelled, and then find the residual driving term (indices p, q).

To begin, recall that Eqn (2.2) also describes the wire-corrector coefficient (Introduction):

$$c_{pq}^{\mathrm{w,R}} = N^{\mathrm{w,R}} \frac{\beta_x^{\mathrm{w},R\,\frac{p}{2}} \beta_y^{\mathrm{w},R\,\frac{q}{2}}}{\left|\mathsf{D}_x^{\mathrm{w},R}\right|^{p+q}} \tag{2.6}$$

and similar for "L". Here $N^{\mathrm{w,R}}$, an effective charge, is proportional to the integrated current of the wire. Repeating the same steps as for (2.3), the contribution of two wires, both installed at distance D^{w} and with the same $N^{\mathrm{w}} = N^{\mathrm{w,L}} = N^{\mathrm{w,R}}$, to the RDT is

$$\Sigma_{pq}^{\mathrm{w}} = N^{\mathrm{w}} (\psi_{\mathrm{w,L}}^{-p} \psi_{\mathrm{w,R}}^{-q} + \psi_{\mathrm{w,R}}^{-p} \psi_{\mathrm{w,L}}^{-q}) \tag{2.7}$$

where $r \equiv \sigma_{\mathrm{w,R}}/\sigma_{\mathrm{w,L}}$, $\psi \equiv \psi_{\mathrm{w,L}} = \frac{\mathsf{D}^{\mathrm{w}}}{\sigma_{\mathrm{w,L}}}$, $\psi_{\mathrm{w,R}} = \frac{\mathsf{D}^{\mathrm{w}}}{\sigma_{\mathrm{w,R}}}$. Here quantities ψ and r now take values within the wire domain on Figure 1.

The cancellation condition is

$$\Sigma_{p_1,q_1} + \Sigma^{\mathrm{w}}_{p_1,q_1} = 0$$
$$\Sigma_{p_2,q_2} + \Sigma^{\mathrm{w}}_{p_2,q_2} = 0. \tag{2.8}$$

Omitting the derivation, we write the solutions of (2.8). For this, define the following functions of r

$$A(r) \equiv \frac{\Sigma_{pq}}{(r^p + r^q)} = \sum_{n\in \mathrm{bb}} \psi_n^{-(p+q)} \frac{r_n^p + r_n^q}{r^p + r^q} \tag{2.9}$$

and correspondingly $A_1(r) \equiv \dfrac{\Sigma_{p_1q_1}}{(r^{p_1} + r^{q_1})}$, $A_2(r) \equiv \dfrac{\Sigma_{p_2q_2}}{(r^{p_2} + r^{q_2})}$. Introduce also

$$P_1 = p_1 + q_1, \;\; P_2 = p_2 + q_2$$

and require that $P_1 \neq P_2$. With these two definitions, the solutions are:

1) for the effective charge (it depends only on r):

$$N^{\mathrm{w}}(r) = (A_1^{-P_2} A_2^{P_1})^{\frac{1}{P_1 - P_2}}; \tag{2.10}$$

2) for the wire distance to axis (depends on r and the components $\sigma_{\mathrm{w,L}}$ of $\boldsymbol{\sigma}$):

$$\mathrm{D}^{\mathrm{w}} = \sigma_{\mathrm{w,L}} \, (A_1^{-1} A_2)^{\frac{1}{P_1 - P_2}}. \tag{2.11}$$

The solutions (2.10) and (2.11) are identical to the ones in [1]: taking some sample p_1, q_1, p_2, q_2 and values of r within the wire domain produces identical plots, see Figure2.

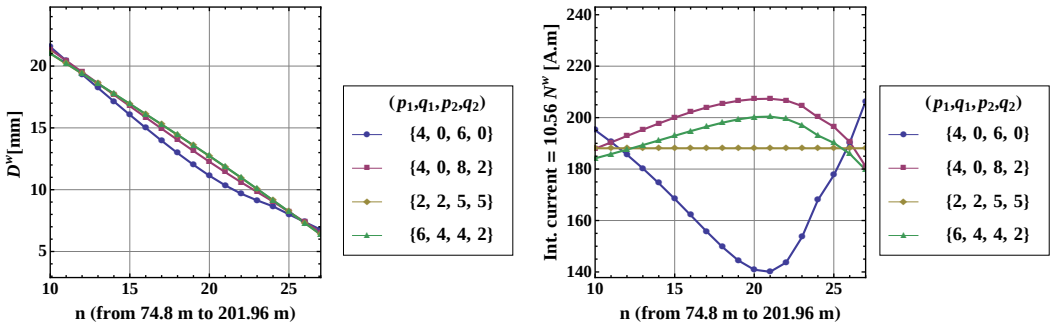

FIG. 2. Eqns (2.11) and (2.10) tabulated for several pairs coefficients over the wire domain - to be compared with Fig 5 in [1].

3) for the residual uncorrected RDT (it depends only on r):

$$\text{With } \; h \equiv (A_1^{-1}A_2)^{\frac{-P}{P_1-P_2}}\,(r^p + r^q),$$

$$R_{pq}(r) = N^{\rm w} h - \Sigma_{pq} =$$

$$= A_1^{-\frac{P_2-P}{P_1-P_2}}\; A_2^{\frac{P_1-P}{P_1-P_2}}\; (r^p + r^q) - \Sigma_{pq}, \tag{2.12}$$

where $P \equiv p+q$. Expression (2.12) again agrees with the results in [1]. For example, by using some of the corrected pairs p_1, q_1, p_2, q_2, Figure 3 shows $|R_{pq}|$ as a function of r^2 for all (p,q) (for all orders 5 and 10).

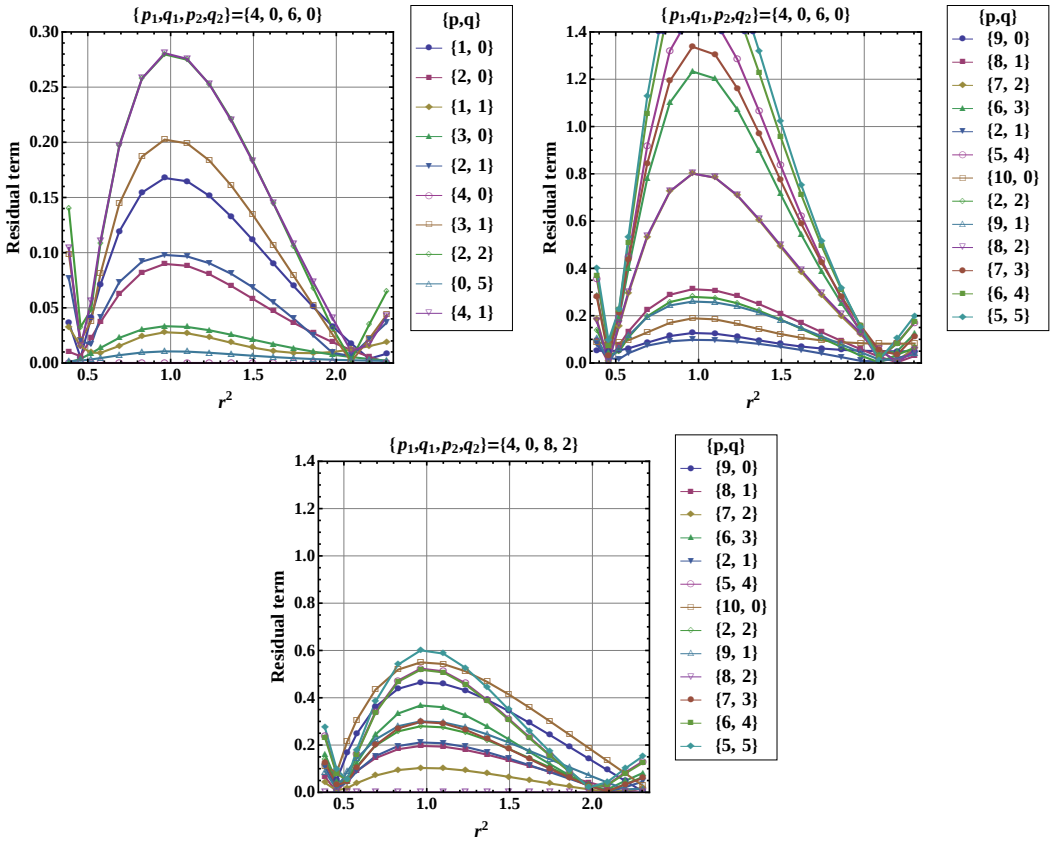

FIG. 3. Dependence on r^2 of the residual driving term, Eqn (2.12), to be compared with Fig 7 in [1].

The meaning of Figures 2 and 3, i.e. of the last three equations, is as follows. If two wires with parameters $N^{\rm w}(r_{\rm w})$ and $\mathsf{D}^{\rm w}(r_{\rm w})$ are installed at symmetric locations where the aspect ratio is $r = r_{\rm w}$ (the left wire is at ratio $1/r_{\rm w}$), then $\Sigma_{p_1q_1}$ and $\Sigma_{p_2q_2}$ are cancelled at these locations. With wires thus installed, the dependence of any residual p,q-driving term on r is for any r given by (2.12).

An inspection of the figures shows that, for the sample triads chosen: (p_1,q_1,p_2,q_2) and (p,q), there are indeed special locations where both r_w^2 and r^2 are near $1/2$ and 2. The question is why

this may be true for nearly every such triad (and clarify the meaning of "nearly").

C. Equation for the special aspect ratios

The special aspect ratios r, for which the residuum term (2.12) as also cancelled, satisfy the equation $R_{pq}(r) = 0$. From (2.9) and (2.12), the equation describing them is

$$A_1(r)^{-\frac{P_2-P}{P_1-P_2}} A_2(r)^{\frac{P_1-P}{P_1-P_2}} = A(r). \tag{2.13}$$

If (p_1, q_1, p_2, q_2) are not too large, then the (only) two roots can be found numerically (it proves best to take the logarithm of both sides) and as we have seen they are near $1/\sqrt{2}$ and $\sqrt{2}$. For large such indices, this becomes difficult.

The symmetry of (2.13) implies some properties of its roots. If r is a solution, then notice that in (2.13) the powers of A are related; there are the identities:

$$\frac{P_2-P}{P_1-P_2} + P_2\frac{P_1-P}{P_1-P_2} = P. \tag{2.14}$$

First, an inspection of (2.13), the definitions of RDT (2.4), and of A (2.9), shows that if r is a solution, then $1/r$ is also a solution (the signs of all p_i, q_i, P_i are reversed).

Second, by using again (2.14), it can be checked that if there is only a single bb collision occurring at flatness parameter r_n (the sum contains only a single term), then the solution is simply $r = r_n$ (and $r = 1/r_n$) – optimum wire is at the same flatness as the sole l.r.

D. Explanation of the appearance of special ratios

Assume that there is a solution r of (2.13) valid for any triad of indices. Introduce, along with the sum $P = p + q$, also the difference $M = p - q$ (a measure the coupling). We are now looking for r such that (2.13) is fulfilled for arbitrary both P and M.

To begin with P, notice that for (2.13) to be true for any P, it is sufficient that A is of the form:

$$A = S^P \tag{2.15}$$

(and hence $A_1 = S^{P_1}$, $A_2 = S^{P_2}$). This again follows from (2.14).

On the other hand, the expression for A (2.9) can be rewritten as

$$A = \sum_{n\in \mathrm{bb}} V_n^P; \;\; V_n \equiv \left(\psi_n^{-1} \frac{r_n^{(P+M)/2} + r_n^{(P-M)/2}}{r^{(P+M)/2} + r^{(P-M)/2}} \right)^{1/P}. \tag{2.16}$$

The quantity S is the so called "p-norm" [2] of the vector $\boldsymbol{V} = (V_1, V_2, \dots)$:

$$S = \left(\sum_{n \in \text{bb}} V_n^P \right)^{1/P}. \tag{2.17}$$

Importantly, the components V_n (they depend on the lattice parameters in the bb region) satisfy the following: for $M < P$ the dependence of V_n on r is nearly the same for all n. This is illustrated on Figure 4.

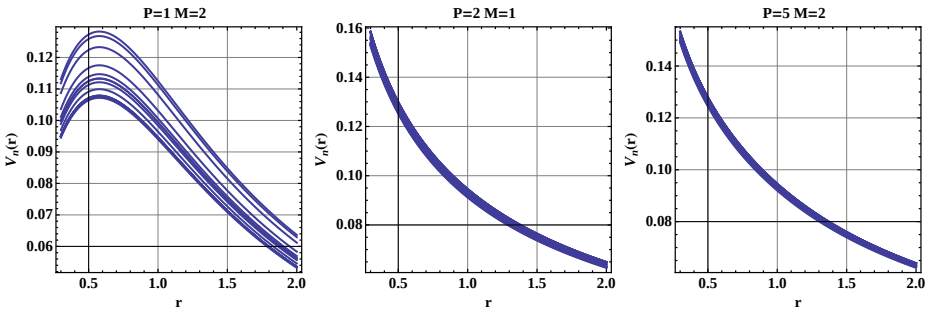

FIG. 4. Curves $V_n(r)$ for the 18 l.r. collisions in IR5 Right. When $M < P$, they overlap, i.e. $V_n(r)$ becomes nearly independent of n.

At this point we only know that the solution r valid for any P exists if $A = S^P$ where S is a p-norm. Next, M must be also arbitrary, so S should not depend on M. Require therefore that the derivative of S over M is zero and use the chain rule:

$$\frac{dS}{dM} = \frac{d}{dM} \left(\sum_{n \in \text{bb}} V_n^P \right)^{1/P} = 0$$
$$\frac{dS}{dM} = \frac{1}{PS^{P-1}} \sum_{n \in \text{bb}} \frac{d}{dM} V_n^P = \frac{1}{S^{P-1}} \sum_{n \in \text{bb}} V_n^{P-1} \frac{dV_n}{dM} = 0$$

Since V_n^{P-1} is almost independent of n, it can be taken outside the sum so the equation for r becomes

$$\sum_{n \in \text{bb}} \frac{dV_n}{dM} = 0. \tag{2.18}$$

Here the signs of the terms are important as for some n they may cancel.

In practice, (2.18) is solved by minimizing the absolute value of left-hand side. The conclusion is that finding the minimum of the p-norm of a vector over the parameter M can, at least in our case, be done by minimizing the modulo of sum of derivatives of its components.

By taking the derivatives of V_n (2.16), the condition (2.18) finally becomes

$$\sum_{n\in \mathrm{bb}} \frac{1}{2P\psi_n} \left(\frac{(r_n^{-\frac{1}{2}(M+P)} r^{\frac{1}{2}(M-P)} (r_n^M+1)}{r^M+1} \right)^{\frac{1}{P}} \times \left(-\frac{r_n^M-1}{r_n^M+1} \log r_n + \frac{r^M-1}{r^M+1} \log r \right) = 0. \tag{2.19}$$

This equations (2.18) and the following from it (2.19) have been derived under the assumption that (2.13) has the same solution r for any triad. They are valid for $M < P$. Differently from (2.13), for arbitrary P and M their roots can easily be found numerically. Studying the dependence of the roots on P and M should then answer to question "nearly all triads", see above:

1) When M is varied, but is small, the roots are with accuracy 10^{-2} equal to $1/\sqrt{2}$ and $\sqrt{2}$, but gradually deviate as M increases. By taking r_n and ψ_n from Table (2.5), this is illustrated on Figures 5 which show the dependence on r for both the individual $\frac{dV_n}{dM}(r)$ and their average $\frac{1}{18} \times \frac{dV_n}{dM}(r)$ (the dashed curve).

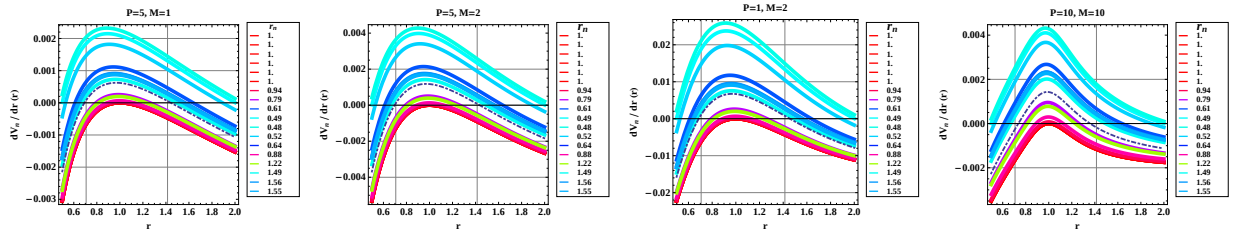

FIG. 5. Several arbitrary values of P and M. Derivatives (2.19) and their average (black dashed) depending on r. The average is seen to be close to zero near the two magic ratios $1/\sqrt{2}$ and $\sqrt{2}$ (black vertical lines) and deviates for larger M. Individual curves are colored with $\mathtt{Hue[n]} = r_n$.

2) when P exceeds several units, the (only) two roots of (2.19)are (as expected) independent of P. To explain this, note that in limit $P \to \infty$, (2.19) becomes

$$\sum_{n\in \mathrm{bb}} \psi_n^{-1} \left(\frac{r_n^M-1}{r_n^M+1} \sqrt{r_n} \log r_n - \frac{r^M-1}{r^M+1} \sqrt{r} \log r \right) = 0. \tag{2.20}$$

For (2.20) to hold, P only needs to exceed several units, say $P \geq 4$. For such P, with regard to obtaining the same roots, equation (2.20) is equivalent to (2.19).

E. Dependence on the long-range flatness parameters via weight function

As it turns out, the special locations depend on the flatness parameters r_n, but not on the normalized separations ψ_n (at least for the sample lattice considered).

To show this, an approximate equation of r is derived as follows. Define an average $<\psi_n^{-1}>$ with $\sum_{n\in \mathrm{bb}} \psi_n^{-1} = N_{bb} <\psi_n^{-1}>$. Then (2.20) becomes

$$\sum_{n\in \mathrm{bb}} \psi_n^{-1} \frac{r_n^M - 1}{r_n^M + 1} \sqrt{r_n} \log r_n = N_{bb} <\psi_n^{-1}> \frac{r^M - 1}{r^M + 1} \sqrt{r} \log r. \tag{2.21}$$

Further, for r within $0.5 < r < 2$, the square root may be ignored: $\sqrt{r}\log r$ can be replaced with $\log r$, and if we also approximately replace $\psi_n^{-1} \approx <\psi_n^{-1}>$, then (2.20) is equivalent to

$$\sum_{r_n \neq 1} F_M(r_n) = N_{bb} F_M(r), \text{ where } F_M(r) \equiv \frac{r^M - 1}{r^M + 1} \log r. \tag{2.22}$$

Here still $N_{bb} = 18$, but since $F_M(1) = 0$, the summation is only over the "flat" collisions. The F_M has the meaning of a weight function: the solution r is such that the value of F_M at r equals the average contributions of all collisions taken with a weights $F_M(r_n)$. In other words, F_M shows how much the flatness at the beam-beam collision contributes to the magic root. It is seen to depend on the coupling parameter M. (It also has its analogy in the problem of approximating an integral with the value of the integrand at some point.)

If the exact curves on Figure 5 are replaced the approximate ones, the roots are preserved. The approximate curves that follow from (2.22) $\sum_{r_n\neq 1} F_M(r_n) - N_{bb} F_M(r) = 0$ are plotted on Figure 6 for comparison with Figure 5. When M is small, the error thus made (in finding r) is again $\sim 10^{-2}$.

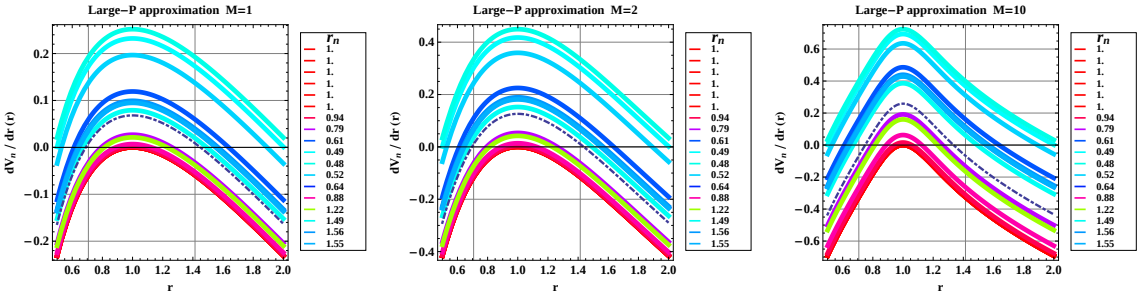

FIG. 6. Same as Figure 5, but for the approximation (2.22).

F. Subsets of long-range collisions

We have shown that for all $N_{bb} = 18$ l.r. collisions, the roots of (2.18) and its approximation (2.22) nearly equal $1/\sqrt{2}$ (and inverted), this being the case for arbitrary triads of indices when M is small.

The above remains true to the same degree for some appropriate subsets of l.r. collisions (subsets of r_n) – say for $N_{bb} = 3, 6$. If there was only a single bb collision present occurring at ratio

r_n, then, as mentioned above, the solution is $r = r_n$ (and $r = 1/r_n$). In the same time, a fundamental property of the p-norm is that for large P it can be replaced by the maximum (modulo) of its elements.

$$\lim_{P \to \infty} S = \max_{1 \le n \le 18} |V_n|. \tag{2.23}$$

One may then speculate that the sum in (2.18) is for large P well represented by appropriate subsets of n. I.e., they produce the same roots as all of the 18. An indication for this is that on Figure 5, there are three well separated groups of curves: the top one mostly representing $r_n \sim 1/2$, the middle one – $r_n \sim 3/2$, and the bottom one – the (overlapping) red ones with $r_n \approx 1$.

Such appropriate subsets turn out to be a mix of several round-beam l.r. with l.r. positioned near the extremes: $r_n \approx 1/2$ or $r_n \approx 3/2$ (see (2.5)). The observations is that these subsets "produce" the special roots, while the effect of the rest tends to cancel near the magic roots – Figure 7.

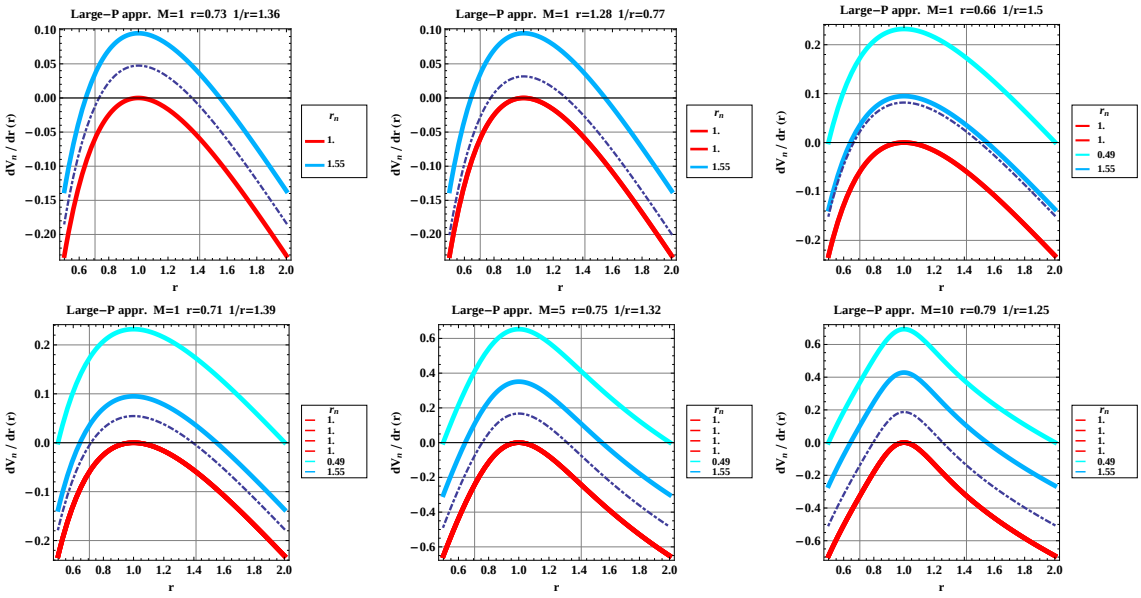

FIG. 7. As on Figure 6 but for several subsets containing increasing number of round ($r_n = 1$) l.r. bb collisions and a fixed number flat ones. For the flat ones, r_n are taken near the extreme values ($r_n \approx 1/2$, or $r_n \approx 3/2$). When there are two round ones per flat one, the roots (shown on top) are very close to $\sqrt{2}$ or $1/\sqrt{2}$. Again this behaviour is violated for large M.

Thus the specific value $r \approx \sqrt{2}$ may be explained with the flatness being $\approx \sqrt{2}$ and $\approx 3\sqrt{2}$ for l.r. collisions near the extremes of the aspect parameter in the beam-beam region.

3. CONCLUSIONS

By deriving equation (2.12) for the residuum driving term, the paper confirms the findings in [1]. Namely, it follows from this equation that for small $M = p - q$ (stronger coupling) the lattice locations at which multiple driving terms are cancelled by the wire correspond to the special (magic) values of the flatness parameter reported in [1]. It is further found that the same equation, combined with the properties of the p-norm of a vector, explains the mechanism of appearance of special values.

A simple weight function is proposed to measure the contribution of an individual collision to the optimum flatness parameter at the wire, Eqn (2.22). It could be further used to predict how the special locations depend on the IR optics and number of long range collisions.

The specific value $r \approx \sqrt{2}$ may, for the sample HL-LHC lattice taken, be explained with the flatness being $\approx \sqrt{2}$ and $\approx 3\sqrt{2}$ for l.r. collisions near the extremes of the aspect parameter in the beam-beam region.

---

[1] S. Fartoukh, A. Valishev, Y. Papaphilippou, D. Shatilov, *Compensation of the long-range beam-beam interactions as a path towards new configurations for the high luminosity LHC*, Phys. Rev. ST Accel. Beams 18, 121001 (2015)

[2] `P-norm` in mathworld.wolfram.com/VectorNorm